Volatile fatty acids recovery from the effluent of an acidogenic digestion process fed with grape pomace by adsorption on ion exchange resins

Published Version:
Volatile fatty acids recovery from the effluent of an acidogenic digestion process fed with grape pomace by adsorption on ion exchange resins / Rebecchi, Stefano; Pinelli, Davide; Bertin, Lorenzo; Zama, Fabiana; Fava, Fabio; Frascari, Dario. - In: CHEMICAL ENGINEERING JOURNAL. - ISSN 1385-8947. - STAMPA. - 306:(2016), pp. S1385894716310476.629-S1385894716310476.639. [10.1016/j.cej.2016.07.101]

Availability:
This version is available at: https://hdl.handle.net/11585/562676 since: 2016-09-13

Published:
DOI: http://doi.org/10.1016/j.cej.2016.07.101

(Article begins on next page)

Volatile fatty acids recovery from the effluent of an acidogenic digestion process fed with grape pomace by adsorption on ion exchange resins

Stefano Rebecchi[1], Davide Pinelli[1], Lorenzo Bertin[1*], Fabiana Zama[2], Fabio Fava[1], Dario Frascari[1]

[1]*Department of Civil, Chemical, Environmental and Materials Engineering, University of Bologna, Via Terracini 28, 40131 Bologna, Italy*

[2]*Department of Mathematics, University of Bologna, Piazza di Porta S. Donato 5, 40100 Bologna, Italy*

** Corresponding author: Lorenzo Bertin*

email: lorenzo.bertin@unibo.it

Tel: *+39 051 20 90317*

Fax: *+39 051 20 90322*

Keywords: Amberlyst A21; amino resin; volatile fatty acids; solid phase extraction; ion exchange model; desorption

Abstract

The purpose of this work was to perform the preliminary development and optimization of a volatile fatty acid (VFA) separation process from an actual effluent of grape pomace acidogenic anaerobic digestion by ion exchange (IE) resins. Batch IE and desorption tests were performed with acetic acid, VFA synthetic mixtures and an actual digestate. The comparison of four amino IE resins led to the selection of Amberlyst A21, a tertiary amino resin characterized by a relatively low price and high IE performances. The latter increased by increasing VFA chain length, this suggesting a relevant contribution of physical adsorption for high molecular weight VFAs. The best IE performances were obtained at pH 3-4.5 in the presence of acetic acid alone, and at pH 6.5 with the actual digestate. Basified ethanol allowed a complete desorption of all the adsorbed VFAs. Solvent recovery by evaporation, obtained with negligible losses of the desorbed VFAs, allowed the production of a highly concentrated water solution of the recovered VFAs. This result represents a crucial feature for the development of innovative VFA-fed biotechnological processes such as polyhydroxyalkanoate production ones. A model taking into account VFA IE, the competitive effect exerted by other anions and the HCO_3^-/CO_3^{2-} buffering effect that characterizes actual digestates led to a satisfactory prediction of the experimental data, and represents an effective tool to identify the optimal operational conditions. Overall, Amberlyst A21 represents an effective candidate for the development of an adsorption / desorption process for VFA recovery from the effluents of acidogenic fermentations.

List of symbols

$[A^-]$	ion acetate concentration at the equilibrium (mol/L)
$[A]_0$	acetic acid concentration initially supplied to the batch system (mol/L)
$[Cl^-]$	chloride ions concentration at the equilibrium in the liquid (mol/L)
$[CO_2]$	absorbed CO_2 concentration in the liquid (mol/L)
$[CO_3^{2-}]$	carbonate concentration in the liquid (mol/L)
$[H^+]$	protons in solution concentration the equilibrium in the liquid (mol/L)
$[H_2CO_3]$	carbonic acid concentration in the liquid (mol/L)
$[HA]$	acetic acid concentration at the equilibrium (mol/L)
$[HCO_3^-]$	bicarbonate concentration in the liquid (mol/L)
$[Na^+]$	sodium ions concentration at the equilibrium in the liquid (mol/L)
$[OH^-]$	hydroxy groups concentration at the equilibrium in the liquid (mol/L)
$[R_3N]$	resin amino groups concentration at the equilibrium in the liquid (mol/L)
$[R_3N]_0$	resin amino groups concentration initially supplied to the batch system (mol/L)
$[R_3NAH]$	group amino-ion acetate concentration at the equilibrium in the liquid (mol/L)
$[R_3NH^+]$	protonated resin amino groups concentration at the equilibrium in the liquid (mol/L)
$C_{calc,i}$	i^{th} calculated concentration, for the calculation of the correlation coefficient (mol/L)
$C_{exp,i}$	i^{th} experimental concentration, for the calculation of the correlation coefficient (mol/L)
$C_{exp.m}$	average value of the experimental concentrations in a given test, for the calculation of the correlation coefficient (mol/L)
$C_{L,A}$	acetic acid concentration in the liquid (mol/L)
$C_{L,A,eq}$	total acetic acid concentration in the liquid at equilibrium (mol/L)
$C_{L,VFA,0}$	initial VFA concentrations in the liquid (mmol/L)
$C_{L,VFA,eq}$	final VFA concentrations in the liquid (mmol/L)
$C_{S,A}$	sorbed concentration of acetic acid (mmol/$g_{dry\ resin}$)
$C_{S,A,\infty}$	sorbed acetic acid concentration at saturation, in the Langmuir model (mmol/$g_{dry\ resin}$)
$C_{S,A,eq}$	sorbed acetic acid concentration in the solid at equilibrium (mmol/$g_{dry\ resin}$)
$C_{S,VFA,eq}$	VFA concentration in the solid at equilibrium (mmol/$g_{dry\ resin}$)
H_{CO2}	Henry constant for the absorption of CO_2 in water (29.76 atm L/mol)
$k_{a,A}$	acetic acid dissociation constant (1.8 10^{-5} mol/L)
$k_{a1,CO2}$	first dissociation constant of carbonic acid ($2.52 \cdot 10^{-4}$ mol/L)
$k_{a2,CO2}$	second dissociation constant of carbonic acid ($5.64 \cdot 10^{-11}$ mol/L)
$k_{b,R}$	basic equilibrium constant of the resin (mol/L)
$k_{h,CO2}$	CO_2 hydration constant = $1.70 \cdot 10^{-3}$ (-)
$k_{s,RA}$	equilibrium constant of the resin-acetic acid salt (L/mol)
k_W	dissociation constant of water (10^{-14} mol^2/L^2)
$mol_{VFA,initial}$.	moles of VFAs in the liquid before the adsorption test
$mol_{VFA,sorbed}$	moles of VFAs sorbed by the resin
m_{resin}	dry resin mass ($g_{dry\ resin}$)
P_{CO2}	CO_2 partial pressure in the gas phase (atm)
$V_{L,added}$	liquid volume added to the resin (mL)
$V_{L,final}$	final liquid volume (mL)
X_p	vector of the simulated equilibrium concentrations in the Gauss Newton method
y	vector of the experimental data, in the Gauss Newton method
Y_{ads}	adsorption yield, calculated as $mol_{VFA,sorbed} / mol_{VFA,initial}$ (-)
ϑ_A	adsorption equilibrium constant of acetic acid in the Langmuir model (mol/L)
ϕ	vector of the experimental conditions used for the best fit of the proposed model
θ	vector of unknowns in the best fitting

1. Introduction

Volatile fatty acids (VFAs) are important bio-based chemicals, which can be produced through anaerobic digestion (AD) processes carried out under acidogenic conditions [1]. VFAs can represent precursors for the production of biopolymers, biofuels and chemicals such as esters, ketones, aldehydes, alcohols and alkanes. Thus, their recovery from liquid effluents of anaerobic acidogenic digestion (AAD) processes becomes attractive in the perspective of approaching the so called "carboxylate platform" [2]. The AAD of agro-industrial waste could represent an effective and competitive approach for the production of VFAs. Therefore, the production of highly concentrated VFAs effluents from biowastes and their subsequent separation is of interest in the perspective of obtaining valuable products from wastes [3,4].

Grape pomace (GP) is the most plentiful solid waste originated by the winemaking process. 3.2 Mtons of GPs were produced in Europe in 2013 [5]. In the past they were mostly used for ethanol production in distilleries. Recently, alternative disposal methods and applications started to be applied, such as thermovalorisation [6] or the production of animal feed [7], compost and fertilizers [8,9]. Furthermore, GP carries a particularly high concentration of tannins and phenolic compounds, whose antioxidant features make their recovery industrially attractive and widely studied [4,10]. GP is characterized by a significant amount of organic carbon, mainly composed by cellulose (14% ± 3%), hemicellulose (13% ± 7%) and lignin (33% ± 8%) [3]. GP AD is an interesting way to convert the organic carbon into energy. However, low specific biomethanization yields were generally obtained (120-270 NL_{CH4}/kg_{VS} [11,12]). Several explanations were proposed for this evidence, such as the high amounts of slowly-fermentable lignin and the inhibitory effects due to the occurrence of alcohols and polyphenols [12]. While biomethane production from GP appears to be not competitive, its anaerobic digestion could be of interest if it is truncated before methanogenesis, so as to produce a VFA mixture. In order to curb methane production and to promote VFA accumulation, high organic loading rates in the 5-15 $kg_{COD}/(m^3\ d)$ range are required, whereas the optimal retention time are in the 1-7 d range [13].

VFA recovery from the acidogenic broth is the main obstacle to their utilization. In fact, a multiple phase separation and enrichment process is generally required in order to obtain marketable products from effluents of biomass transformation processes. In particular, a well-established "5-Stages Universal Recovery Process" was proposed for the recapture of valuable compounds from food waste [14]. Many VFA recovery methods have been evaluated. Liquid-liquid extraction, based on the use of specific anionic extracting agents (such as organophosphates and aliphatic amines) in solvents, is characterized by high efficiencies and easy application, but it is not environmentally friendly [15]. In electrodialysis (ED), VFAs are carried across a membrane, from a solution to another, thanks to the application of a voltage difference between two electrodes [16]. High membrane cost, high energy demand, membrane fouling, back diffusion and polarization represent the main problems of the ED approach. Nanofiltration, a pressure-driven membrane separation based on size and electrical interactions, shows a high selectivity towards VFA. However, it is characterized by high membrane cost and energy demands, and it does not lead to the production of highly concentrated VFA solutions [17].

VFA adsorption and ion exchange (IE) are based on the interaction between the carboxylate groups of solved VFAs and the active sites of a solid matrix. In particular, while adsorption is based on a physical interaction between the adsorbent and the protonated neutral form of the VFA, IE is based on the formation of ionic bond between the ionized acid and a cation, such as an ammonium salt, which represents the functional group of the commonly used anionic IE resin. This technology represents an interesting approach for VFA recovery, since the adsorbent can be directly applied into the effluent and easily separated from it. Adsorption can be effectively applied for the recovery not only of VFAs [18] but also of other added-value compounds occurring in organic effluents, such as polyphenols [19,20]. Most works reported in the literature on organic acids adsorption are applied towards the products of pure-culture fermentations, such as succinic, lactic and formic acids

[21,22,23]. Other studies focused on the adsorption of synthetic VFA mixtures on resins [24,25]. For example, Kim et al. [26] studied the ability of amino-functionalized mesoporous silica nanoparticles to adsorb synthetic solutions of different carboxylic acids. pH, temperature and the presence of coexisting chemicals were tested, and a maximum capacity of 3.4 $mol_{VFA}/kg_{dry\ resin}$ was reached when acetic acid was used alone.

A limited number of studies investigated the integrated adsorption/desorption process on single VFAs (acetic, propionic, butyric acid) and mixtures of them. For example, Silva and Miranda [27] compared the adsorption performances of a weak base resin (Purolite A133S) with those of activated carbon, and identified n-propanol as the optimal eluent for the desorption process. VFA adsorption from actual fermentation effluents was investigated by few studies [28,29]. However, these works were aimed at removing VFAs from the fermentation broth in order to avoid inhibitory effects, and not at recovering them. Therefore, the application of this technology to actual acidogenic effluents is still poorly developed.

Finally, although IE is a well-established separation method, the process modelling focused mainly on wastewater treatment applications, with a particular emphasis on metals and cations adsorption [30,31].

The mechanism of IE of an acid on a primary, secondary or tertiary amine is described by the following equilibria:

$$HA \leftrightarrows A^- + H^+ \quad (1)$$

$$R_xNH_{3-x} + H_2O \leftrightarrows R_xNH_{4-x}^+ + OH^- \quad (2)$$

$$R_xNH_{4-x}^+ + A^- \leftrightarrows R_xNH_{4-x}A \quad (3)$$

where HA indicates the carboxylic acid, A^- the carboxylate anion, R_xNH_{3-x} the non-protonated amine (with $x = 1$ for a primary amine, 2 for a secondary amine and 3 for a tertiary amine), $R_xNH_{4-x}^+$ the protonated amine and $R_xNH_{4-x}A$ the acid-resin salt. In case of a quaternary ammonium salt IE resin, which is always positively charged independently on pH, reaction (2) does not apply and $R_xNH_{4-x}^+$ is the correspondent ammonium cation. Reactions (1) to (3) clearly show the marked dependency on the pH of the process of VFA IE on a resin. Indeed, for a primary, secondary or tertiary amine a pH increase determines on the one hand a stronger IE as a result of the increase of the ionized form of the acid, but on the other hand a lower IE due to the decrease of the protonated form of the amine. Therefore, an optimal intermediate pH is expected. Conversely, in case of a quaternary amine a pH increase leads only to the first effect (higher IE due to a higher concentration of ionized acid).

This work had the general aim to perform the preliminary development and optimization of a process of VFA separation by adsorption on IE resins from an effluent of GP acidogenic anaerobic digestion. The specific goals were: (i) to select the most suitable IE resin among four tested ones; (ii) to test and calibrate a simplified IE model, capable to predict the effect of pH on VFA IE on the selected resin; (iii) to optimize the adsorption step in terms of pH; and (iv) to optimize the desorption step in terms of solvent and pH. The tests aimed at selecting the resin and optimizing the adsorption / desorption process (goals i, iii and iv) were performed with actual GP AAD effluent, whereas the development of the VFA IE model and the tests aimed at its calibration were carried out with acetic acid, selected as a representative VFA. Finally, the ability of the model to predict the IE of VFAs from an actual GP AAD effluent was tested.

The main novelties of this work are (i) the study of VFA IE from an actual VFA-rich waste stream, instead of a synthetic solution, (ii) the optimization of the VFA desorption step, generally neglected in the previous studies on VFA adsorption, (iii) the testing and calibration of a simplified IE model aimed at studying the effect of pH on the adsorption step and (iv) the development of a method to produce a highly concentrated solution of VFAs in water, suitable for further downstream processes.

2. Material and methods

2.1. Materials and VFA-rich effluent production

Four IE resins were tested in this work: Sepra NH2 (primary amine), Ambelyst A21 (tertiary amine), Sepra SAX and Sepra ZT SAX (quaternary amine). Their main chemical-physical characteristics and their price are reported in Table 1. Before the experiments, each resin was conditioned as illustrated by the supplier.

Single VFAs were purchased from Sigma Aldrich. The GP employed in this work was kindly provided by the "Il Glicine" winery (Cesena, Italy) and it was obtained by processing "Sangiovese" red vines. GP anaerobic digestion was aimed at producing a VFA-rich effluent. The GP, that initially contained 41.8% of total solids (TS), was thermally pre-treated at 55°C in order to increase its digestibility. The dried GP was re-suspended in de-ionized water and mixed to an acclimated acidogenic inoculum (10% v/v), so as to obtain at the beginning of the batch anaerobic digestion a TS content equal to 17%. This value corresponds to a semi-solid process that curbs methanogenesis, thus driving the fermentation towards acidogenesis. The GP AAD was carried at 37°C, and the pH was controlled at 7 [32]. After 21 days the supernatant was separated from the solid by centrifugation (4000 rpm, 15 min) and further filtered at 0.2 µm to completely remove micro solids in suspension. The VFA composition and the total COD of the filtered effluent is reported in Table 2. The COD due to VFAs, equal to 27.7 g/L, is equal to 85% of the total COD of the digestate.

2.2 Analytical methods

Volatile Fatty Acids were analyzed by an Agilent GC-FID (model 7890A) equipped with an Agilent J&W GC column, 30 m x 0,25 mm x 0,25 µm (injection volume 1 µl; injector temperature 250°C; column initial temperature 80 °C; 0.5 min isotherm; first temperature rate 20°C/min to 150 °C for 1 min; second temperature rate 20°C/min to 240°C for 2.5 min; detector temperature 280°C). Before GC-FID analysis, the samples were diluted with an oxalic acid solution (60 mM) in the ratio

1:4. COD was determined spectrophotometrically using COD Vario Tube Test (Aqualytic, Dortmund, Germany).

2.3 General experimental approach

All the adsorption and desorption experiments were carried out in batch mode, in vials containing either 1 or 50 mL of VFA-rich liquid phase (depending on the specific test) and a liquid / dry resin ratio equal to 25 mL/g. Each experiment was conducted in triplicate. The vials were shaken at 150 rpm and room temperature (20-22 °C). Preliminary tests characterized by frequent analysis indicated that, under these experimental conditions, the liquid / solid equilibrium was reached after 60-90 minutes. The batch tests were therefore stopped after 120 minutes. After separation of the liquid phase from the resin, and the VFA concentrations in the liquid was determined. The sorbed VFA concentrations at equilibrium, $C_{S,VFA,eq}$, were then calculated as $C_{S,VFA,eq} = (C_{L,VFA,0} \cdot V_{L,added} - C_{L,VFA,eq} \cdot V_{L,final}) / m_{resin}$, where m_{resin} is the dry resin mass, $C_{L,VFA,0}$ and $C_{L,VFA,eq}$ are the initial and final VFA concentrations in the liquid, whereas $V_{L,added}$ and $V_{L,final}$ are respectively the liquid volume (filtered GP digestate, or synthetic solution of VFAs in water) added to the resin and the final liquid volume, taking into account the water added with the resin.

2.4 Resin selection tests

Two sets of batch tests were performed to select the most effective resin among the four tested ones (Table 1; assay n. 1). These tests were conducted with 0.04 g of dry resin and 1 mL of either GP acidogenic digestate (first set of tests) or a synthetic solution of acetic acid (20 g/L, equal to the total VFA mass concentration in the GP acidogenic digestate) in de-ionized water (second set of tests). The adsorption performances of the tested resins were compared in terms of adsorption yield (Y_{ads}), calculated as $mol_{VFA,sorbed} / mol_{VFA,initial}$.

2.5 Development and calibration of a pH-dependent VFA ion exchange model

One of the goals of this work was to test and calibrate a simplified IE model capable to simulate the effect of pH on the IE of acetic acid, selected as a representative VFA, on the best performing resin (Amberlyst A21). Indeed, traditional sorption models, such as the Langmuir one, generally do not include the effect of pH, and are therefore not suitable to describe the IE of acids on amine-functionalised resins. On the other hand, previous attempts to simulate the IE of acids led to the development of complex models, based on the electrical double layer theory and involving a high number of parameters [24,33,34]. To this goal the following model was utilized, based on the equilibrium of reactions (1), (2), (3), on the acetic acid and resin mass balances and on the charge balance, and referred to the specific case of a tertiary amine:

$$k_{a,A} = [A^-] \cdot [H^+]/[HA] \quad (4)$$

$$k_{b,R} = [R_3NH^+] \cdot [OH^-]/[R_3N] \quad (5)$$

$$k_{s,RA} = [R_3NHA]/([R_3NH^+] \cdot [A^-]) \quad (6)$$

$$k_W = [OH^-] \cdot [H^+] \quad (7)$$

$$[A]_0 = [A^-] + [HA] + [R_3NHA] \quad (8)$$

$$[R_3N]_0 = [R_3N] + [R_3NH^+] + [R_3NHA] \quad (9)$$

$$[R_3NH^+] + [H^+] + [Na^+] = [A^-] + [OH^-] + [Cl^-] \quad (10)$$

$$k_{s,RCl} = [R_3NHCl]/([R_3NH^+] \cdot [Cl^-]) \quad (11)$$

where $[A]_0$ and $[R_3N]_0$ indicate respectively the concentrations of acetic acid and resin amino groups initially supplied to the batch system, whereas all the other concentrations refer to the final equilibrium condition. All the concentrations are referred to the final volume of liquid phase, including the free, protonated and bonded amino groups. In Eq. (5) the basic dissociation constant of the resin ($k_{b,R}$) is defined so as to include the water concentration. The sorbed concentration of acetic acid referred to the dry resin mass was eventually calculated as $C_{S,A} = [R_3NHA] \cdot V_{L,final} / m_{resin}$, as $[R_3NHA]$ indicates the sorbed concentration referred to the liquid volume. In Eq. (10) (charge balance), $[Na^+]$ and $[Cl^-]$ are added in order to include the general case in which the system pH is corrected through the addition of a completely dissociated base (NaOH) or acid (HCl): in the isotherm tests no NaOH or HCl were added, but in subsequent tests (section 2.6) these compounds were added in order to test the capacity of the model to predict the IE capacity of the selected resin at different pH values. Similarly, Eq. (11) takes into account the competitive IE effect exerted by Cl^- when HCl is added to correct the pH.

In a second phase of work, the proposed model was modified in order to predict the pH behaviour of IE tests conducted with an actual GP digestate. Indeed, in this case the relevant carbonate and bicarbonate concentrations associated to the presence of CO_2 in the headspace determine in a buffering effect. Thus the HCl concentration required to attain a given pH, and therefore the Cl^- competitive effect, are significantly higher than in the acetic acid / water system, where no buffering effect occurs. To simulate this effect, the liquid phase concentrations of CO_2, H_2CO_3, HCO_3^- and CO_3^{2-} were simulated according to the following equilibrium equations:

$$H_{CO_2} = P_{CO_2}/[CO_2] \tag{12}$$

$$k_{h_{CO2}} = [H_2CO_3]/[CO_2] \tag{13}$$

$$k_{a_{1,CO_2}} = ([H^+] \cdot [HCO_3^-])/[H_2CO_3] \tag{14}$$

$$k_{a_{2,CO_2}} = ([H^+] \cdot [CO_3^{2-}])/[HCO_3^-] \tag{15}$$

where P_{CO2} indicates the CO_2 partial pressure in the gas phase and H_{CO_2} Henry's constant for the absorption of CO_2 in water. The charge balance was modified to take into account all the CO_2 ionic forms:

$$[R_3NH^+] + [H^+] + [Na^+] = [A^-] + [OH^-] + [Cl^-] + [HCO_3^-] + 2 \cdot [CO_3^{2-}] \tag{16}$$

In order to calibrate the first part of the model (Eqs. (4-10), without Cl^- competitive effect on acetic acid IE), the ion exchange of acetic acid on the best performing resin was studied by means of 2 isotherm tests, conducted according to the general procedure illustrated in section 2.3, at different initial concentrations of acetic acid in the 17-330 mmol/L range (1-20 g/L; assay n. 2). This range was determined so as to have a maximum acetic acid mass concentration about equal to the VFA mass concentration of the GP acidogenic digestate (Table 2). The 2 isotherm tests were conducted respectively with 1 and 50 mL of acetic acid solution in water, in order to evaluate possible scale effects and to reduce the uncertainty in the estimation of the unknown parameters $[R_3N]_0$, $k_{b,R}$ and $k_{s,RA}$. The tests were monitored by measuring the final pH and acetic acid concentration in the liquid phase ($[A^-]$ + $[AH]$), and by calculating the corresponding solid phase concentrations $C_{S,A}$.

The model equations (4-10) were used to estimate the unknown parameters $[R_3N]_0$ (total concentration of amino groups in the resin), $k_{b,R}$ (basic equilibrium constant of the resin) and $k_{s,RA}$ (equilibrium constant of the resin-acetic acid salt), represented below by vector θ, applying best fitting approximation of the isotherm experimental data obtained for each specific experimental condition tested (i.e. for each initial acetic acid concentration $[A]_0$ and liquid phase volume V_L, equal to 1 or 50 mL). Indicating the 11 tested experimental conditions with vector $\phi = (\phi_1, \dots, \phi_p, \dots, \phi_{11})$, the correspondent experimental data (y_p) were obtained for each experiment p by measuring the pH and the total acetic liquid phase ($[A^-]$ + $[AH]$), and by calculating the sorbed $C_{s,A}$ from the experimental data. For each experiment p and for each parameter vector θ, Eqs. (4-11) were rewritten as a system of nonlinear equations:

$$F(X_p, \theta, \phi_p) = 0, \quad p = 1, \dots, 11 \tag{17}$$

where each solution vector X_p indicates the equilibrium concentrations ($[A^-]$, $[AH]$, $[R_3NH^+]$, $[R_3N]$, $[R_3NAH]$, $[OH^-]$, $[H^+]$) in a given experimental condition p. The following constant values were used: $k_{a,A} = 1.8 \cdot 10^{-5}$ M, $k_W = 10^{-14}$ M, $[Na^+] = [Cl^-] = 0$, as no HCl or NaOH were added in the isotherm tests.

The estimation of the parameter vector θ was performed by minimizing the sum of the weighted squared deviations between the experimental data y_p and the corresponding simulated values. A dedicated Matlab function was implemented to compute the solution vectors X_p of (17) on the basis of the built-in non-linear solver *fzero*. On the basis of the experimental data, we assigned suitable initial guesses to the parameter vector ($\theta^{(0)}$) and - for each experimental condition p – to the equilibrium concentrations ($X_p^{(0)}$). The least square problem was solved by means of a dedicated Matlab code that implements the Gauss Newton algorithm, following the procedure illustrated by [35] and later adapted to convection-dispersion problems by Zama et al. [36]. The best fitting value of the parameter vector θ was estimated by means of an iterative approach. As a convergence criterion, the iterations k were stopped when the mean relative parameter variation ρ_k resulted $< 10^{-3}$, where ρ_k was defined as follows:

$$\rho_k = \sum_{j=1}^{j=3} \left| \frac{\vartheta_j^{(k)} - \vartheta_j^{(k-1)}}{\vartheta_j^{(k)}} \right| \tag{18}$$

Although $[R_3N]_0$ could be theoretically estimated by multiplying the active site concentration in the resin provided by the supplier (expressed as mmol/$g_{\text{dry resin}}$) by the resin concentration in the tests (40 $g_{\text{dry resin}}$/L), in the case of Amberlyst A21 this approach leads to an underestimate of the actual $[R_3N]_0$ value, as the supplier provides only the lower limit of the active site concentration range (> 4.6 mmol/$g_{\text{dry resin}}$).

For comparison purposes, the experimental values of total acetic acid concentration in the liquid ($C_{L,A,eq}$, equal to $[A^-] + [HA]$) and of sorbed acetic acid concentration ($C_{S,A,eq}$) relative to the isotherm tests (without any acid or base addition) were also interpolated by means of the Langmuir sorption model:

$$C_{S,A,eq} = \frac{C_{S,A,\infty} \cdot C_{L,A,eq}}{\beta_A + C_{L,A,eq}} \qquad (19)$$

Acetic acid was selected as a representative VFA as it constitutes 2/3 of the total VFA molar concentration in the GP acidogenic digestate (Table 2). To evaluate whether the IE behaviour of acetic acid on Amberlyst A21 is really representative of that of VFA mixtures, a third isotherm (assay n. 3) was performed with a synthetic VFA mixture characterized by roughly the same total VFA massic concentration of the real digestate and by a VFA composition close to that of the real digestate, except for the absence of isobutyric and isovaleric acid and for a higher concentration of propionic acid (Table 2). The differences between the synthetic VFA mixture and the VFA composition of the actual GP digestate are due to the fact that the isotherm performed with the synthetic mix was utilized also in other studies performed with different type of acidogenic digestates, characterized by different VFA profiles. In this isotherm, conducted with 1 mL of liquid phase, the VFA mixture was tested at different concentrations in the 14-271 mmol/L range (1-19.1 g/L of VFA).

The quality of each best fit was evaluated by means of the correlation coefficient R^2, defined so as to allow the comparison of models with different numbers of parameters [37]:

$$R^2 = 1 - \left(\frac{\sum_{i=1}^{N} \left(C_{\exp,i} - C_{calc,i} \right)^2}{N - P - 1} \right) \Bigg/ \left(\frac{\sum_{i=1}^{N} \left(C_{\exp,i} - C_{\exp,m} \right)^2}{N - 1} \right) \qquad (20)$$

where N indicates the number of experimental data and P the number of parameters evaluated by best fit on the experimental data.

2.6 Effect of pH variations on the IE of acetic acid and of the GP acidogenic digestate

A further test (assay n. 4) was conducted with 1 mL of acetic acid solution in water (333 mM, or 20 g/L) in order to assess the effect of pH variations by means of HCl or NaOH additions on the performance of IE of acetic acid on the selected resin, as well as the capacity of the above-described IE model (Eqs. (4-11)) to predict such effect. In 4 sets of triplicate vials, before adding the selected resin the spontaneous pH of the 20 g/L acetic acid solution (equal to 2.4) was changed respectively to 1.29 (by adding 60 mM of HCl), 1.08 (HCl 100 mM), 4.99 (NaOH 220 mM) and 7.14 (NaOH 340 mM). Then 100 mg of Amberlyst A21 (40 mg of dry resin) were added, and after 2 hours the tests were monitored by measuring the final pH and acetic acid concentration in the liquid phase. The experimental VFA aqueous and solid phase concentrations were compared with the corresponding theoretical ones obtained with Eqs. (4-11), providing the added amounts of Cl^- or Na^+ as inputs, in order to evaluate the capacity of the proposed model to predict the effect of pH and the Cl^- competitive on acetic acid IE on the selected resin. To this purpose, the equilibrium constant of the reaction of formation of the resin-Cl salt ($k_{s,RCl}$) was evaluated by best fit on the experimental data, according to the procedure illustrated in section 2.5 for the estimate of the other model parameters.

To test the effect of pH on the IE of the VFAs contained in an actual GP acidogenic digestate on Amberlyst A21, the IE of 1 mL of filtered digestate was tested at the optimal pH of the anaerobic digestion process (pH=7) and at initial pH values (before resin addition) equal to 5 and 2.5, by adding suitable amounts of HCl (assay n. 5). The experimental VFA aqueous and solid phase concentrations were compared with the corresponding theoretical ones predicted by the extended version of the model (Eqs. (4-16)), providing the added amounts of Cl^- as inputs.

2.7 Identification of the optimal solvent for the desorption step

To identify the optimal solvent for VFA desorption from the best performing resin, 6 tests of VFA IE from 1 mL of pH 5 GP acidogenic digestate were operated in triplicate, with Amberlyst A21 (assay n. 6). After reaching the liquid-solid equilibrium, the liquid phases were replaced with 1 mL of 6 alternative desorption solvents: ultrapure H_2O, ultrapure H_2O + NaOH 1M, 99% pure ethanol (EtOH), EtOH + NaOH 1M, EtOH + NaOH 0.1M, EtOH + NaOH 0.01M. After shaking the vials for 2 h at 150 rpm and at room temperature, VFA concentration in the liquid phase was measured.

2.8 Resin adsorption performances in repeated adsorption cycles

In order to assay the effect of the adsorbent reuse on adsorption performances, the same resin was exposed to three consecutive adsorption cycles (assay n. 7). Each single cycle experiment was conducted in triplicate using 1 mL of a synthetic solution of 10 g/L of acetic acid and 0.04 g of the best performing resin (Amberlyst A21). After 1.5 hours of 150 rpm shaking at room temperature, the liquid was collected and replaced with 1 ml of the best desorption solvent, according to the results related to assay n. 6. The vials were shaken at 150 rpm for 1 hour in order to desorb acetic acid. Finally, the solvent was collected and the resin was washed with de-ionized water in order to remove the desorption solvent and the residual acetic acid.

3. Results and discussion

3.1. Resin selection

Table 1 reports the sorbed concentrations and adsorption yields (Y_{ads}) obtained in the resin selection tests conducted with the actual GP digestate (pH 7) and with a synthetic solution of 20 g/L of acetic acid in water (pH 2.7) (assay n. 1). Amberlyst A21 clearly outperformed the other 3 resins in both selection tests. Considering also that the price of Amberlyst A21 is 3.5-47 times lower than that of the other 3 tested resins, the former was selected for the subsequent tests.

For all the tested resins the sorption performances obtained with the actual digestate were significantly lower than the corresponding values obtained with acetic acid, and in the case of Sepra NH2 VFA sorption even dropped to zero when the actual digestate was tested. This finding can be ascribed to the effect of pH, to its change caused by adsorption and to the presence in the GP digestate of a relevant concentration of non-VFA COD (about 5 g_{COD}/L; Table 2), that is likely to exert a competitive effect on VFA sorption. Considering that acetic acid represents 67% of the molar concentration of VFAs in the tested digestate (Table 2), it is unlikely that the observed 2-6 fold drop in sorption performances can be due to a lower affinity of the four resins for the other VFAs present in the tested VFA mix.

Amberlyst A21 is a weakly basic polymeric resin. The capacity of this kind of resins to separate organic acids was widely studied [18, 23]. Importantly, Amberlyst A21 was also selected among other polymeric resins for the detoxification of Beet distillery effluent from acetic acid and other organic acids by Fargues et al.[28].

3.2. Development and calibration of a pH-dependent VFA ion exchange model

The experimental data relative to the two isotherms conducted with acetic acid (1 mL and 50 mL of aqueous phase; assay n. 2) are shown in Figs. 1a (solid phase versus aqueous phase concentrations) and 1b (pH versus aqueous phase concentrations). Figs 1a and 1b show also the best-fitting simulation obtained with the proposed model (Eqs. (4-11)). The simulated data are reported both as single points corresponding to the experimental conditions, in order to show the deviation between experimental and simulated data, and as a continuous line, in order to compare the proposed model (Eqs. (4-10), without Cl^- competitive effect) with the Langmuir isotherm (shown in Fig. 1a with a hatched line). The Gauss-Newton algorithm used to calibrate the proposed model converged after 6-7 iterations. The best-fitting values of the unknown parameters of the proposed model ($[R_3N]_0$, $k_{b,R}$, $k_{s,RA}$) and of the Langmuir model ($C_{S,A,\infty}$ and β_A) are reported in the caption of Fig. 1. The best estimate of $[R_3N]_0$ (0.22 M, corresponding to 5.6 mmol/$g_{dry\ resin}$) corresponds to a total concentration of amino groups in the resin 22% higher than the minimum guaranteed value reported by the supplier (4.6 mmol/$g_{dry\ resin}$). The 2 isotherms performed with acetic acid, with 1 mL and 50 mL of aqueous phase, were in very good agreement with each other. The proposed IE model allowed a very good overall fit of the experimental acetic acid concentrations in the liquid phase ($R^2 = 99.7\%$) and in the solid phase ($R^2 = 99.5\%$), and a fairly good fit of the experimental pH values ($R^2 = 80.4\%$). As shown in Fig. 1a, the proposed model led to a simulated curve of solid phase versus aqueous phase acetic acid concentration very close to that obtained by a best fit of the Langmuir model (Eq. (19)), with an average deviation between the 2 curves equal to 5.5%.

The experimental acetic acid concentrations in the solid and liquid phase relative to the isotherm conducted with the synthetic VFA mixture (Table 2, assay n. 3) are shown in Fig. 1c, together with the simulated curve produced with Eqs. (4-10) and calibrated on the 2 isotherms performed with only acetic acid. It can be observed that the proposed IE model, calibrated on only acetic acid, leads to a very good prediction of the total VFA sorbed concentrations for liquid phase VFA concentrations > 10 mM (average relative deviation = 4%). For liquid concentrations < 10 mM the proposed model is characterized by a less accurate prediction (relative deviations in the 20-30% range), probably due to the lower precision of the experimental GC method at low VFA concentrations.

The overall adsorption yield of the VFA mixture, calculated from the highest concentration test for each VFA, resulted very close to that of the tests with only acetic acid (65% versus 61%, respectively). The capacity of the IE model calibrated on acetic acid to predict the IE behaviour of the VFA mixture can be explained by considering that the pK_a values – and therefore the acid strengths – of VFAs in the C2-C7 range are very close to each other (Table 2). This observation suggests that, in the interaction between C2-C7 VFAs and Amberlyst A21, IE prevails on physical adsorption on the polymeric matrix. However, the examination of the adsorption yields relative to the single VFAs suggests that physical adsorption could play a significant role in the case of the longer-chain VFAs. Indeed the single VFA Y_{ads} increased significantly from 62-63% of acetic and propionic acid to 85% of caproic acid (Table 2). Differences in the selectivity of similar IE resins towards C2-C4 VFAs was also observed by Kim et al. [26], Silva and Miranda [27] and Fargues et al. [28]. These differences in Y_{ads} could be explained by the strongly increasing trend of the VFA octanol/water partition coefficient (K_{ow}) versus chain length (Table 2). Indeed K_{ow}, often used to estimate the adsorption constants of organic pollutants on organic sorbents [38], increases by more than 2 orders of magnitude in the C2-C7 VFA range.

Lastly, it can be observed in Fig. 1c that the experimental solid phase concentrations of acetic acid (that represents in molar terms 58% of the VFA mixture) fall significantly below the corresponding predicted concentrations (calibrated on the isotherm performed with only acetic acid). This indicates that, in the VFA mixture isotherm, C3-C7 acids exert a relevant competitive effect on the IE of acetic acid.

3.3 Effect of pH variations on the IE of acetic acid and of the GP acidogenic digestate

HCl and NaOH were used to study the effect of pH correction on the IE of acetic acid in a synthetic solution (assay 4). The experimental data are shown in Figs. 2a (solid phase versus aqueous phase concentrations) and 2b (pH versus aqueous phase concentrations). Figs 2a and 2b also show the best-fitting simulation obtained with the proposed model, including both the cases of Cl^- competitive effect on acetic acid IE (Eqs. (4-11)) and that of no Cl^- competitive effect (Eqs. (4-10)). The simulated data are reported both as single points using as inputs the experimental additions of HCl or NaOH reported in section 2.6 and as complete simulated lines.

The experimental data show that both acidification and basification determined a marked decrease in the IE of acetic acid on Amberlyst A21. The solid phase concentrations ranged from 0.4 to 4 mmol/$g_{dry\ resin}$, versus 5.3 mmol/$g_{dry\ resin}$ under the same conditions (333 mM initial acetic acid concentration) in the absence of pH correction. Similarly, the adsorption yield (equal to 61% without pH correction) dropped to 35-45% in the case of HCl additions and 7-31% with NaOH additions.

As shown by the semi-hatched line in Fig. 2b, the simulation performed in the absence of competitive IE by any anion (Eqs. (4-10)) leads to a curve of solid phase concentration versus pH characterized by a bell shape, with a broad maximum in the 2.5-4.5 pH range. This result can be explained by considering that, for a tertiary amine, as the pH increases the concentration of the ionized form of the acid A^- increases (reaction (1)), but the concentration of the active protonated amino groups decreases, with opposite effects on the concentration of the amine-acid salt. These findings are in agreement with the results of a study of VFA and polyphenols IE on a resin with a tertiary amine group (IRA 67), where a pH increase from 4.9 to 7.2 determined a decrease in the adsorption yield of both VFA and polyphenols from 60% to 20% [39]. The IE simplified model (Eqs. (4-10), without Cl^- competitive effect) resulted in a fairly high capacity to predict the IE of acetic acid in case of NaOH additions (full vs. empty squares in Fig. 2a and 2b; average relative deviations relative to $C_{S,A}$, $C_{L,A}$ and pH equal to 18%), whereas in case of acidification the model predictions (empty triangles only in Fig. 2b) were unacceptable. This outcome can be explained by considering that Na^+ does not exert any competitive effect on the IE of acetic acid, whereas it is likely that the addition of Cl^- concentrations equal to 18-30% of the acetic acid concentration determines a marked competitive IE of Cl^- on Amberlyst A21. This effect was documented in several previous studies [24,26,29].

To validate this explanation, the competitive IE of chloride was incorporated in the proposed model by adding an additional equilibrium relative to the formation of a $R_xNH_{4-x}Cl$ salt (Eq. (11)). The experimental data of assay 4 (HCl additions to the acetic acid synthetic solution) were used to assess the best fitting value of $k_{s,RCl}$ using the previously optimised $k_{b,R}$, $[\boldsymbol{R_3N}]_{\mathbf{0}}$, and $k_{s,RA}$ values as inputs. The simulated values for assay 4 (empty diamonds in Figs. 2a and 2b) are in very good agreement with the experimental data (full diamonds). The model with Cl^- competitive effect was then used to predict the IE of acetate with increasing HCl additions. On the basis of this simulation, as shown in Fig. 2b (hatched line), the maximum concentration in the solid is achieved in the 3-4.5 pH range, without any HCl addition. Indeed, at pH < 3 the model predicts an abrupt drop in the IE performance as even small amounts of HCl are added. Conversely, at pH > 4.5 the solid phase concentration starts to decrease as a result of the combined effect of acid ionization (reaction (1)) and resin deprotonation (reaction (2)).

The experimental data relative to the tests of GP acidogenic digestate IE on Amberlyst A21 at different pH levels (assay n. 5) are shown in Figs. 2b (solid phase concentration versus pH) and 2c (solid phase versus liquid phase concentration). The GP AD process was maintained at pH 7 by means of NaOH periodic additions in order to maximize the VFA production rate. However, given the poor IE performances obtained with acetic acid in the 6.5-9 pH range, the IE of the VFA-rich GP digestate on the selected resin was tested also at lower initial pH values, equal to 5 and 2.5, by means of HCl additions. For each studied condition, the addition of resin to the actual GP determined a pH increase, leading to final pH values equal to 7.2, 6.5 and 5.2, for the tests with initial pHs of 7, 5 and 2.5 respectively. As shown in Fig. 2b, the qualitative trend of solid phase concentration versus pH was similar to that observed with acetic acid alone: while a decrease in final pH from 7.2 to 6.5 led to a doubling of the solid phase concentration, a further decrease to 5.2 determined a decrease in IE performance, with a solid phase VFA level close to that observed at pH 7.2. The best IE performance was obtained at a final pH equal to 6.5, with a solid phase VFA concentration of 1.4 mmol/$g_{dry\ resin}$ and in relatively good agreement with the value predicted by the model (semi-hatched line in Fig. 2b).

These data were simulated with the complete IE model (Eqs. (4-16)), that includes not only the competitive IE of chloride ions, but also the buffering effect determined by bicarbonates and carbonates. The previous best estimates of $k_{b,R}$, $[\boldsymbol{R_3N}]_{\boldsymbol{0}}$, $k_{s,RA}$ and $k_{s,RCl}$, and the P_{CO2} value measured in the GP digestion tests (0.4 bar), were used as input values. As shown in Fig. 2c, the simulated values (empty symbols) resulted fairly close to the experimental ones (full symbols), with an average deviation equal to 12%.

The adsorption yields obtained in this test relatively to the single VFAs are shown in Table 2. Interestingly, Y_{ads} increased with increasing size of the molecule, indicating a higher affinity of the selected resin for the middle-chain VFAs, characterized by a higher market value. As discussed previously, this trend is probably due to an increasing contribution of physical adsorption, indicated by the increasing K_{ow} values.

Despite the possible competition exerted by other anions present in the GP digestate, the results obtained at a final pH equal to 6.5 indicate that Amberlyst A21 can be effectively utilized to separate VFAs from actual acidogenic fermentation effluents. Two approaches could be envisaged in order to improve the VFA IE performances obtained in this test. The first consists in operating the acidogenic digestion at an acidic pH. Indeed, AAD naturally leads to an acidic pH due to VFA production. This suggests the possibility to find an optimal pH by balancing the increase in VFA IE by Amberlyst A21 obtained at decreasing pH (semi-hatched line in Fig. 2b) and the corresponding decrease in VFA production rate. Indeed, on the basis of preliminary data of GP AAD conducted at different pHs, a pH reduction from 7 to 5 leads to a 40% decrease in VFA production rate. The second approach consists in operating the VFA production process at its optimal pH (7) and then attaining the optimal pH for VFA IE by means of a less competitive acid than HCl. However, this appears to be a complex task, as all the most commonly used inorganic acids are known to compete with acetic acid in IE. For example, Kim et al. [24] and Takahashi et al. [26] showed that sulfuric acid has an interaction with weak IE resins stronger than HCl. Phosphoric acid [24] and nitric acid [29] have behaviors similar to that of HCl.

3.4 Identification of the optimal solvent for the desorption step

In assay 6, after the IE of the pH 5 GP digestate on Amberlyst A21, 6 alternative desorption solvents were tested. The resulting desorption yields, evaluated as (moles desorbed) / (moles adsorbed), are reported in Fig. 3a in terms of overall VFA yield for each tested solvent. While water performed poorly, ethanol led to the desorption of about 2/3 of the sorbed VFAs. This behavior is reasonable if one takes into account that ethanol depresses ionic dissociation equilibria and is a powerful desorption solvent for physically adsorbed compounds [19]. In particular, as shown in Fig. 3b, ethanol led to high desorption yields for all the tested VFAs, whereas in the case of water the desorption yields decreased linearly with increasing number of carbons in the molecule.

For both solvents, the addition of NaOH 1 M (pH = 14) led to a complete desorption. This finding is in agreement with the proposed IE model (reactions (1-3)): indeed an increase in $[OH^-]$ shifts reaction (2) towards the deprotonated form of the amine, reducing the activated form. This, in turn, reduces the concentration of the amine-acid salt, in order to maintain the equilibrium of reaction (3). This behavior was observed also by Kim et al. [26]. According to the experimental data of Fig. 2b, this effect determines in the resin-water system a 92% decrease of the sorbed acetic acid concentration at a pH almost equal to 9. It is therefore reasonable to expect a complete acetic acid desorption in the 10-13 pH range. Thus, the desorption tests were repeated in the presence of NaOH concentrations equal to 0.1 M (pH 13) and 0.01 M (pH 12). These tests were performed only with ethanol, on the basis of the higher desorption performances obtained with ethanol in the absence of NaOH additions and of the significantly lower amount of energy required to evaporate and thus recover ethanol in comparison with water (latent heat of vaporization: ethanol 840 kJ/kg, water 2260 kJ/kg). As shown in Fig. 3a, the decrease in pH led to a corresponding decrease in VFA desorption yield, which reached 80% at a pH equal to 12. Silva and Miranda [27] simulated the application of non-basified ethanol for the desorption of short chain fatty acids from a weakly basic resin, leading to the desorption of 99% of adsorbed acids. However, in that study the volume of eluent necessary for each gram of adsorbed acid was equal to 500 L, which makes the process economically not feasible. Conversely, in this study 1 g of acids was desorbed with 0.2 L of basified ethanol (0.1 M).

With regard to the single VFA desorption yields, Fig. 3b shows that the same decreasing trend with the number of carbon atoms in VFA observed with water is also present in the case of water with NaOH addition, limitedly to the C5-C7 VFAs. On the contrary, in the case of ethanol, regardless of the NaOH concentration, the desorption yields are constant or slightly increasing with VFA size.

In the desorption test performed with ethanol + NaOH 0.1 M the solvent was evaporated, and the residual VFAs were re-suspended in water. This led to a loss of VFA mass equal to just 3% , indicating that when ethanol is used, it is feasible to recycle the desorption solvent and to produce a highly concentrated water solution of the recovered VFAs. This approach can find interesting applications in processes using VFAs as a feedstock and requiring a very high VFA concentration of the feed solution in order to be economically sustainable. A typical example of such processes is polyhydroxyalkanoates production. In this perspective, a relevant issue is represented by the Na^+ concentration in the final VFA-rich solution. Hypothesizing to perform a continuous flow IE process with a 95% sorption yield [19], to desorb with ethanol + 0.1 M NaOH with a 92% desorption yield (Fig. 3a) and to feed a desorption solvent volume equal to 50% of the volume of VFA-rich stream fed to the column [19], the final Na^+ concentration in the desorbed product is equal to about 6% of the VFA concentration, a value that does not determine an excessively high contamination of the final product.

3.5 Resin adsorption performances in repeated adsorption cycles

The adsorption yields obtained by the application of three consecutive adsorption cycles, which were carried out in order to test the possibility of reusing the selected Amberlyst A21 resin (assay 7), resulted almost constant, with variations in the 85%-88% range and standard deviations in the 1%-2% range. The desorption yields resulted in agreement with those obtained in assay 6 with the actual GP digestate, under the same experimental conditions.

4. Conclusions

The comparison of four amino IE resins led to the selection of a tertiary amino resin characterized by a relatively low price, high IE performances in the presence of acetic acid or synthetic VFA mixtures, and acceptable IE performances in the presence of a VFA-rich stream produced by acidogenic digestion of grape pomaces. The IE performances increased with increasing VFA chain length, suggesting a relevant contribution of physical adsorption for high molecular weight VFAs. The best IE performances were obtained at pH 3-4.5 in the presence of acetic acid alone, and at pH 6.5 when real GP digestate was used. Basified ethanol led to a complete desorption of the sorbed VFAs, high desorption yields also for the middle-chain VFAs and an effective solvent recovery by evaporation with negligible losses of the desorbed VFAs.

A relatively simple IE model, taking into account the competitive effect exerted by Cl^- when pH was corrected with HCl, was calibrated on the tests performed with acetic acid / water solutions, and showed a good capacity to predict the IE of a synthetic VFA mixture. The inclusion in the model of the carbonate/bicarbonate buffering effect that occurs in real digestates allowed a fairly good prediction of the IE of a VFAs from a real GP digestate at different pH values. The proposed model thus represents an effective tool to optimize the process of VFA IE from actual digestates.

Overall, this work indicates that Amberlyst A21 represents an effective candidate for the development of an adsorption / desorption process for VFA recovery from the effluents of acidogenic fermentations. This technique could be crucial for the development of other processes that utilize VFAs as a feedstock reagent and that require high concentration VFA solutions, not achievable by acidogenic AD alone. Further research must be performed to develop and optimize the continuous-flow process and to incorporate in the proposed IE model the competitive effects exerted by VFA mixtures and by other anions.

Acknowledgements

Project co-funding by the Italian Ministry of University and Research under PRIN grant "WISE - Turning organic Waste into Innovative and Sustainable End-products" is acknowledged. The authors greatly acknowledge prof. Rita Mazzoni and prof. Enrika Scavetta for their critical feedbacks on the discussion of the data.

References

[1] R.R. Singhania, A. K. Patel, G. Christophe, P. Fontanille, C. Larroche, Biological upgrading of volatile fatty acids, key intermediates for the valorization of biowaste through dark anaerobic fermentation, Bioresource Technol. 145 (2013) 166–174.

[2] M. T. Agler, B. A. Wrenn, S. H. Zinder and L. T. Angenent, Waste to bioproduct conversion with undefined mixed cultures: the carboxylate platform, Trends Biotechnol. 29 (2011) 70–78.

[3] A. Scoma, S. Rebecchi, L. Bertin, F. Fava. High impact biowastes from South European agro-industries as feedstock for second-generation biorefineries, Crit. Rev. Biotechnol. 36 (2016) 175-89.

[4] G.A. Martinez, S. Rebecchi, D. Decorti, J.M.B. Domingos, A. Natolino, D. Del Rio, L. Bertin, C. Da Porto, F. Fava, Towards multi-purpose biorefinery platforms for the valorisation of agro-industrial wastes: production of polyphenols, volatile fatty acids, polyhydroxyalkanoates and biogas from red grape pomace, Green Chem. 18 (2016) 261–270.

[5] FAOSTAT, Food and Agriculture Organization of the United Nations, http://faostat3.fao.org/browse/Q/QC/E 2013 (accessed 11.04.16).

[6] I.S. Arvanitoyannis, D. Ladas, A. Mavromatis, Wine waste treatment methodology, Int. J. Food. Sci. Tech. 41 (2006) 1117–1151.

[7] A. Brenesa, A. Viveros, S. Chamorro, I. Arija, Use of polyphenol-rich grape by-products in monogastric nutrition. A review, Anim. Feed Sci. Tech. 211 (2016) 1–17.

[8] R. Paradelo, A.B. Moldes, M.T. Barral, Evolution of organic matter during the mesophilic composting of lignocellulosic winery wastes, J. Environ. Manage. 116 (2013) 18–26.

[9] M.A. Bustamante, D. Said-Pullicino, C. Paredes, J.A. Cecilia, R. Moral, Influences of winery–distillery waste compost stability and soil type on soil carbon dynamics in amended soils, Waste Manag. 30 (2010) 1966–1975.

[10] M. Ferri, S. Bin, V. Vallini, F. Fava, E. Michelini, A. Roda, G. Minnucci, G. Bucchi, A. Tassoni, Recovery of polyphenols from red grape pomace and assessment of their antioxidant and anti-cholesterol activities, New Biotech. 33 (2016) 338–344.

[11] E. Dinuccio, P. Balsari, F. Gioelli, S. Menardo, Evaluation of the biogas productivity potential of some Italian agro-industrial biomasses. Bioresource Technolo. 101 (2010) 3780–3783.

[12] A. Fabbri, G. Bonifazi and S. Serranti, Micro-scale energy valorization of grape marcs in winery production plants, Waste. Manag. 36 (2015) 156-165.

[13] W.S. Lee, A.S.M. Chua, H.K. Yeoh, G.C. Ngoh, A review of the production and applications of waste-derived volatile fatty acids, Chem. Eng. J. 235 (2014) 83–99.

[15] C.M. Galanakis, Recovery of high added-value components from food wastes: conventional, emerging technologies and commercialized applications, Trends Food Sci. Tech. 26 (2012) 68-87.

[15] E. Alkaya, S. Kaptan, L. Ozkan, S. Uludag-Demirer, G.N. Demirer, Recovery of acids from anaerobic acidification broth by liquid–liquid extraction, Chemosphere. 77 (2009) 1137–1142.

[16] A. Vertova, G. Aricci, S. Rondinini, R. Miglio, L. Carnelli, P. D'Olimpio, Electrodialytic recovery of light carboxylic acids from industrial aqueous wastes, J.Appl. Electrochem. 39 (2009) 2051–2059.

[17] M.P. Zacharof and R.W. Lovitt, Complex Effluent Streams as a Potential Source of Volatile Fatty Acids, Waste Biomass Valor. 4 (2013) 557-581.

[18] C.S. López-Garzón, A.J.J. Straathof, Recovery of carboxylic acids produced by fermentation, Biotechnol. Advances, 32 (2014) 873–904.

[19] D. Frascari, A.E. Molina Bacca, F. Zama, L. Bertin, F. Fava, D. Pinelli, Olive mill wastewater valorisation through phenolic compounds adsorption in a continuous flow column, Chem. Eng. J. 283 (2016) 293–303.

[20] A. Scoma, C. Pintucci, L. Bertin, P. Carlozzi, F. Fava, Increasing the large scale feasibility of a solid phase extraction procedure for the recovery of natural antioxidants from olive mill wastewaters, Chem. Eng. J. 198–199 (2012) 103–109.

[21] C.C. Chen, L.K. Ju, Coupled lactic acid fermentation and adsorption, Appl. Microbiol. Biotechnol. 59 (2002) 170–174.

[22] K. Zhang, S.-T. Yang, In situ recovery of fumaric acid by intermittent adsorption with IRA-900 ion exchange resin for enhanced fumaric acid production by Rhizopus oryzae, Biochem. Eeng. J. 96 (2015) 38–45.

[23] Q. Li, J. Xing, W. Li, Q, Liu, Z. Su, Separation of Succinic Acid from Fermentation Broth Using Weak Alkaline Anion Exchange Adsorbents, Ind. Eng. Chem. Res., 48 (2009) 3595–3599.

[24] V.M. Bhandari, T. Yonemoto, V.A. Juvekar, Investigating the differences in acid separation behavior on weak base ion exchange resins, Chem. Eng. Sci. 55 (2000) 6197-6208.

[25] N. Kanazawa, K. Urano, N. Kokado, Y. Urushigawa, Adsorption Equilibrium Equation of Carboxylic Acids on Anion-Exchange Resins in Water, J. Colloid Interface Sci. 238 (2001) 196–202.

[26] S.H. Kim, Y. Huang, C. Sawatdeenarunat, S. Sung and V.S.Y. Lin, Selective sequestration of carboxylic acids from biomass fermentation by surface-functionalized mesoporous silica nanoparticles, J. Mater. Chem. 21 (2011) 12103–12109.

[27] A. H. da Silva and E. A. Miranda, Adsorption/Desorption of Organic Acids onto Different Adsorbents for Their Recovery from Fermentation Broths, J. Chem. Eng. Data. 58 (2013) 1454−1463.

[28] C. Fargues, R. Lewandowski, M.L. Lameloise, Evaluation of ion-exchange and adsorbent resins for the detoxification of beet distillery effluents, Ind. Eng. Chem. Res. 49 (2010) 9248–9257.

[29] S. Takahashi, K. Tanifuji, K. Shiell, M.S. Jahan, H. Ohi, Y.H. Ni, Removal of Acetic Acid from Spent Sulfite Liquor Using Anion Exchange Resin for Effective Xylose Fermentation with Pichia stipites, Bioresources 8 (2013) 2417-2428.

[30] C. Özmetin, Ö. Aydınb, M.M. Kocakerimb, M. Korkmaza, E. Özmetin, An empirical kinetic model for calcium removal from calcium impurity-containing saturated boric acid solution by ion exchange technology using Amberlite IR–120 resin, Chem. Eng. J., 148 (2009) 420–424

[31] S.H. Lin, C.D. Kiang, Chromic acid recovery from waste acid solution by an ion exchange process: equilibrium and column ion exchange modeling, Chem. Eng. J. 92 (2003) 193–199.

[32] S. Rebecchi, L. Bertin, V. Vallini, G. Bucchi, F. Bartocci, and F. Fava, Biomethane production from grape pomaces: a technical feasibility study, Environ. Eng. Manag. J. 12 (2013) 105–108.

[33] V.M. Bhandari, V.A. Juvekar, S.R. Patwardhan, Sorption Studies on Ion Exchange Resins. 1. Sorption of Strong Acids on Weak Base Resins, Ind. Eng. Chem. Res. 31 (1992) 1060-1073.

[34] V.M. Bhandari, V.A. Juvekar, S.R. Patwardhan, Sorption Studies on Ion Exchange Resins. 2. Sorption of Weak Acids on Weak Base Resins, Ind. Eng. Chem. Res. 31 (1992) 1073-1080.

[35] P. Englezos, N. Kalogerakis, Applied parameter estimation for chemical engineers, Marcel Dekker, New York – Basel, 2001.

[36] F. Zama, R. Ciavarelli, D. Frascari, D. Pinelli, Numerical parameter estimation in models of pollutant transport with chemical reaction, D. Homberg, F. Troltzsch (Eds.), IFIP Advances in Information and Communication Technology, System Modeling and Optimization, Springer, Heidelberg 391 (2013) 547–556.

[37] D. Frascari, S. Fraraccio, M. Nocentini, D. Pinelli, Trichloroethylene aerobic cometabolism by suspended and immobilized butane-growing microbial consortia: a kinetic study, Biores. Technol. 1244 (2013) 529-538.

[38] D. Frascari, A. Zannoni, D. Pinelli, M. Nocentini, Chloroform aerobic cometabolism by butane-utilizing bacteria in bioaugmented and non-bioaugmented soil/groundwater microcosms, Process Biochem. 42 (2007) 1218–1228.

[39] D. Pinelli, A.E. Molina Bacca, A. Kaushik, S. Basu, M. Nocentini, L. Bertin, D. Frascari, Batch and continuous flow adsorption of phenolic compounds from olive mill wastewater: a comparison between non-ionic and ion exchange resins, Int J Chem Eng (2016), in press.

Table 1

Comparison of the tested IE resins: main characteristics, price and VFA sorption performances obtained with acetic acid and with the GP acidogenic digestate. The sorption performances are expressed as average values ± standard deviation in each triplicate experiment.

Resin	Price (€/kg)[a]	Structure	Active sites[b]	Moisture	GP acidogenic digestate test		Acetic acid test	
					$C_{S,VFA}$[c]	Y_{ads}[d]	$C_{S,A}$[c]	Y_{ads}[d]
Sepra NH2	462	Silica primary amine	1.4	0	0	0	1.0±0.1	12%±1%
Amberlyst A21	131	Polymeric tertiary amine	> 4.6	0.6	0.8±0.1	11%±1 %	5.1±0.5	61%±6%
Sepra SAX	502	Silica quaternary amine	0.8	0	0.20±0.05	3%±1%	0.4±0.1	5%±1%
Sepra ZT-SAX	6200	Polymeric quaternary amine	[e]	0	0.20±0.05	3%±1%	1.1±0.1	13%±1%

[a] The reported prices were obtained from the web sites of the resin providers (www.phenomenex.com for Sepra NH2, Sepra SAX and Sepra ZT-SAX; www.sigmaaldrich.com), accessed on March 31, 2016.

[b] $mmol/g_{dry\ resin}$.

[c] Solid phase concentration of acetic acid or VFAs, $mmol/g_{dry\ resin}$.

[d] Acetic acid or VFA adsorption yield ($mol_{VFA,sorbed} / mol_{VFA,initial}$).

[e] Not provided by the resin supplier.

Table 2

GP acidogenic digestate and of the synthetic VFA mixture: composition and adsorption yields obtained in assays 3 and 5.

	Grape pomace acidogenic digestate				Synthetic VFA mixture			pK_a [d]	K_{ow} [d]
	VFA (g/L)	VFA (mmol/L)	VFA (g_{COD}/L) [a]	Y_{ads} (assay n. 5) [b]	VFA (g/L)	VFA (mmol/L)	Y_{ads} (assay n. 3) [c]		
Acetic ac.	11.4	190	12.2	15%	9.5	158	62%	4.75	0.68
Propionic ac.	0.9	12	1.4	18%	3.9	52	63%	4.87	2.1
Isobutyric ac.	0.8	9	1.5	22%	0.0	0		4.84	8.7
Butyric ac.	5.3	60	9.6	24%	3.8	44	72%	4.82	6.2
Isovaleric ac.	0.1	1	0.2	32%	0.0	0		4.78	15
Valeric ac.	0.3	3	0.5	40%	0.9	9	78%	4.84	25
Caproic ac.	1.0	9	2.2	62%	1.0	8	85%	4.88	83
Heptanoic ac.	0.01	0.06	0.02	76%	0.0	0		4.89	263
Total	19.8	284	27.7		19.1	271			

[a] Calculated stoichiometric conversion.

[b] Calculated from the data relative to the best performing test, performed at an initial pH equal to 5.

[c] Calculated from the data relative to the test at the highest concentration, for each VFA.

[d] pK_a and K_{ow} values were obtained from the Open Chemistry Database (https://ncbi.nlm.nih.gov/).

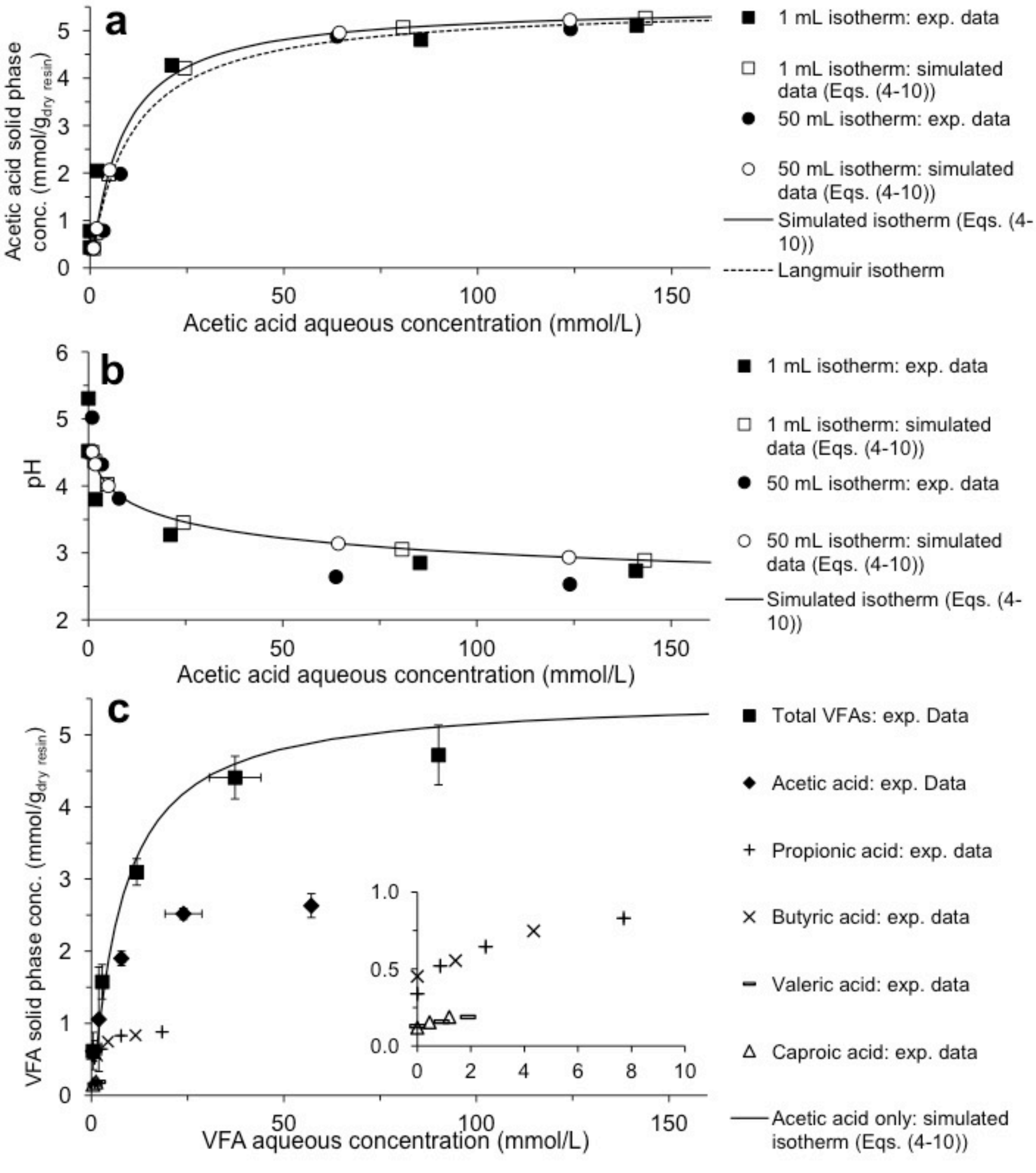

a
Acetic acid solid phase conc. (mmol/g$_{dry\ resin}$)
Acetic acid aqueous concentration (mmol/L)
1 mL isotherm: exp. data
1 mL isotherm: simulated data (Eqs. (4-10))
50 mL isotherm: exp. data
50 mL isotherm: simulated data (Eqs. (4-10))
Simulated isotherm (Eqs. (4-10))
Langmuir isotherm
b
pH
Acetic acid aqueous concentration (mmol/L)
1 mL isotherm: exp. data
1 mL isotherm: simulated data (Eqs. (4-10))
50 mL isotherm: exp. data
50 mL isotherm: simulated data (Eqs. (4-10))
Simulated isotherm (Eqs. (4-10))
c
VFA solid phase conc. (mmol/g$_{dry\ resin}$)
VFA aqueous concentration (mmol/L)
Total VFAs: exp. Data
Acetic acid: exp. Data
Propionic acid: exp. data
Butyric acid: exp. data
Valeric acid: exp. data
Caproic acid: exp. data
Acetic acid only: simulated isotherm (Eqs. (4-10))

Figure 1

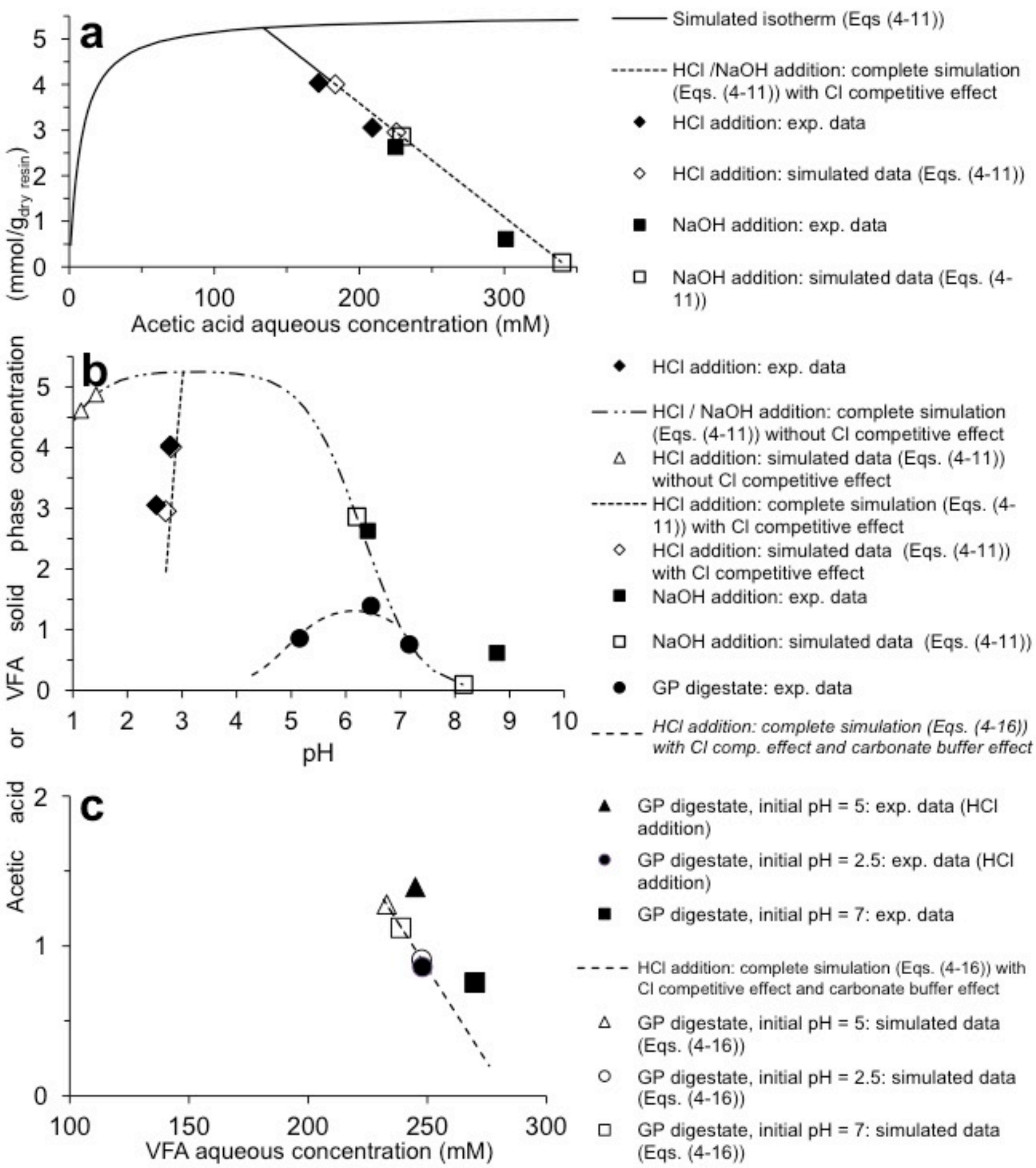
a
Acetic acid aqueous concentration (mM)
Simulated isotherm (Eqs (4-11))
HCl /NaOH addition: complete simulation (Eqs. (4-11)) with Cl competitive effect
HCl addition: exp. data
HCl addition: simulated data (Eqs. (4-11))
NaOH addition: exp. data
NaOH addition: simulated data (Eqs. (4-11))
b
pH
HCl addition: exp. data
HCl / NaOH addition: complete simulation (Eqs. (4-11)) without Cl competitive effect
HCl addition: simulated data (Eqs. (4-11)) without Cl competitive effect
HCl addition: complete simulation (Eqs. (4-11)) with Cl competitive effect
HCl addition: simulated data (Eqs. (4-11)) with Cl competitive effect
NaOH addition: exp. data
NaOH addition: simulated data (Eqs. (4-11))
GP digestate: exp. data
HCl addition: complete simulation (Eqs. (4-16)) with Cl comp. effect and carbonate buffer effect
Acetic acid or VFA solid phase concentration (mmol/g$_{dry\ resin}$)
c
VFA aqueous concentration (mM)
GP digestate, initial pH = 5: exp. data (HCl addition)
GP digestate, initial pH = 2.5: exp. data (HCl addition)
GP digestate, initial pH = 7: exp. data
HCl addition: complete simulation (Eqs. (4-16)) with Cl competitive effect and carbonate buffer effect
GP digestate, initial pH = 5: simulated data (Eqs. (4-16))
GP digestate, initial pH = 2.5: simulated data (Eqs. (4-16))
GP digestate, initial pH = 7: simulated data (Eqs. (4-16))

Figure 2

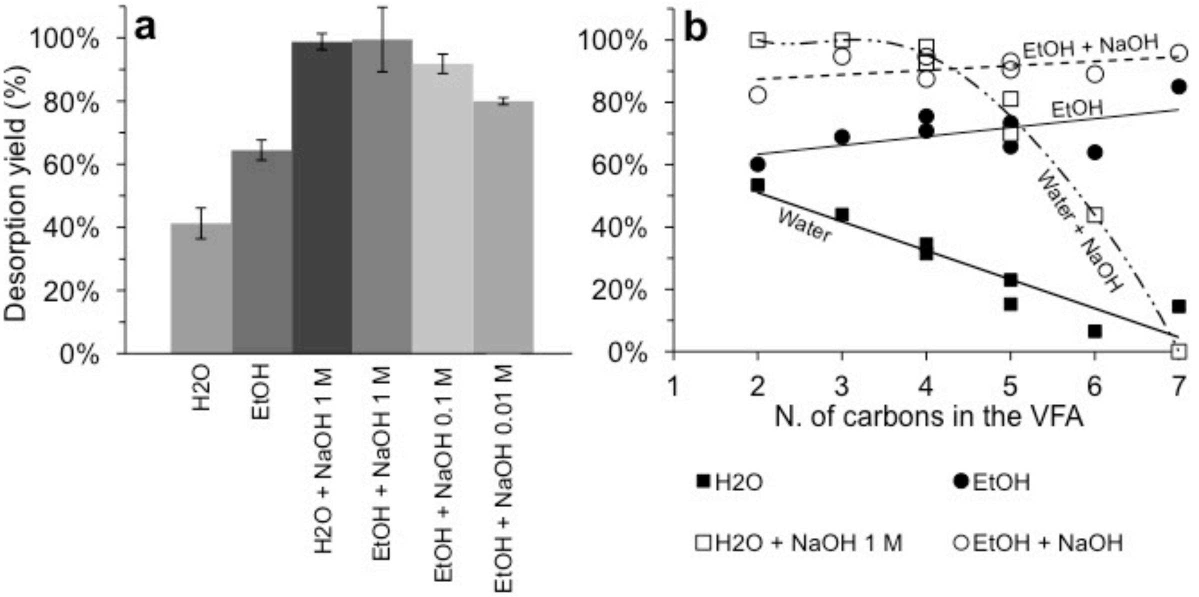

a
Desorption yield (%)
100%
80%
60%
40%
20%
0%
H2O
EtOH
H2O + NaOH 1 M
EtOH + NaOH 1 M
EtOH + NaOH 0.1 M
EtOH + NaOH 0.01 M
b
EtOH + NaOH
EtOH
Water
Water + NaOH
1
2
3
4
5
6
7
N. of carbons in the VFA
H2O
EtOH
H2O + NaOH 1 M
EtOH + NaOH

Figure 3

775